Thermochimica Acta 524 (2011) 151–156

Contents lists available at ScienceDirect

Thermochimica Acta

journal homepage: www.elsevier.com/locate/tca

Kinetic study on the chlorination of indium oxide

F.M. Túnez[c], P. Orosco[a], J.A. González[a,c], M. Del C. Ruiz[a,b,*]

[a] Instituto de Investigaciones en Tecnología Química, INTEQUI, CONICET, INTEQUI, Chacabuco y Pedernera 5700, San Luis, Argentina
[b] Facultad de Química, Bioquímica y Farmacia, Universidad Nacional de San Luis, INTEQUI, Chacabuco y Pedernera 5700, San Luis, Argentina
[c] Instituto de Ciencias Básicas, Universidad Nacional de Cuyo, 5500 Mendoza, Argentina

ARTICLE INFO

Article history:
Received 25 April 2011
Received in revised form 5 July 2011
Accepted 7 July 2011
Available online 18 July 2011

Keywords:
Chlorination
Indium oxide
Kinetic

ABSTRACT

In this paper, the chlorination of In_2O_3 has been studied using gaseous chlorine as chlorinating agent. The results of the thermodynamic analysis for the reaction of In_2O_3 chlorination indicate that this reaction is possible throughout the entire studied temperature range. The progress of the chlorination was followed measuring the mass changes for isothermal and non-isothermal experimental assays. The effect of temperature, reaction time, flow rate and partial pressure of Cl_2 was investigated. The solids were characterized by scanning electron microscopy (SEM) and X-ray diffractometry (XRD). The results of the chlorination assays showed that the reaction between In_2O_3 and Cl_2 starts approximately at 400 °C, with a mass loss of 50% at 620 °C, and that, for temperatures between 500 and 650 °C, the reaction rate increases along with the reaction temperature. The calculated values for the apparent activation energy and for the order of reaction were 125.5 kJ/mol and 0.91, respectively. The model $1-(1-\alpha)^{0.4}=Kt$ is the best represents the experimental data.

1. Introduction

Indium was discovered by F. Reich and T.H. Richter in 1863; later on, they were able to isolate the metal. Until 1924, the world consumption of this element was little and sporadic. Nowadays, around 40 tons of indium are annually produced worldwide, 10 of which are provided by Canada [1,2].

Indium is mostly applied to the production of alloys, such as low melting point alloys (solder alloys), fusible indium alloys, dental alloys and conductive alloys. It is also used in the manufacturing of dry alkaline batteries as a substitute for mercury, in low pressure sodium lamps, in liquid crystal displays, and in intermetallic compounds as GaInAs, GaInP, InP and InSb which are applied to the semiconductors industry (lasers, photodetectors, integrated circuits, and infrared video cameras and detectors) [2].

Indium does not occur in native state and it is widely spread in nature, generally in very low concentrations. The content of this metal in the earth crust is estimated in 0.1 ppm, and it is found in several minerals as trace element. Indium is mainly associated with zinc materials, being sphalerite the ore with the biggest amount of indium; copper and lead sulphides are next in the list. During the recovery process of the base metals, indium concentrates in the residues and the processes for its recovery and purification are often quite complex and inefficient [2]. Even though electro refining is a commonly used technique to obtain high purity indium, additional procedures are needed to comply with the purity grade requirements for this metal in the electronic industry [3]. This is the reason why the development of new methodologies for the recovery and purification of indium is of great importance.

The production of high purity Ga, In and Cd for electronic applications has been studied by Ohwa et al. [4], using a chloride refining process. Nishihama et al. [5] have studied the recovery of In and Ga using liquid–liquid extraction with D_2EHPA, reaching a 98.9% effectiveness for In and 87.9% for Ga [5].

Waste management of materials containing metals, is an issue of increasing importance and attention in mineral and metallurgical industries. This is due mainly to two factors, an urge to reduce environmental problems, and the economic need to optimize the use of non renewable resources. Sustainable development lies on the productive use of human and material resources, and extractive metallurgy represents a promising area for development in this respect.

Although there exist a number of methods for the production of high purity metals, liquid–liquid extraction from metallic halides in solution and the distillation of chlorides are the two most widely used techniques. In both cases, the obtainment of metallic halides constitutes the first stage in the process.

The use of chlorination to recover and refining metals may increase in the future. This is due to a number of factors, which include the high chlorination rates resulting from the elevated reactivity of Cl_2 and other chlorinating agents; the comparatively moderate temperature involved in the chlorination process; the

* Corresponding author. Tel.: +54 2652423789; fax: +54 2652426711.
E-mail addresses: mruiz@unsl.edu.ar, axarquia77@gmail.com (M. del C. Ruiz).

0040-6031/$ – see front matter © 2011 Elsevier B.V. All rights reserved.
doi:10.1016/j.tca.2011.07.007

low cost, variety and availability of chlorinating agents; the favorable physical and chemical characteristics of certain metals; the properties of many chlorides (high solubility, wide variety of oxidation states and ease of separation by liquid–liquid extraction or distillation); the selectivity of the treatment and separation processes; and the development of certain corrosion resistant materials used for the manufactures of reactors [6]. On the other hand, the wastes from chlorination processes can be conveniently treated for the recovery of toxic materials, prior to their final disposal. At present, the use of chlorination for indium recovery is being studied, specially from materials or disposals residues that contain it [7–9].

The kinetics of chlorination of pure In_2O_3 with gas chlorine has been investigated in the present work. Knowledge of the effect of different variables upon the system reactivity may allow to proposing a mechanism and a kinetic reaction model that represent the experimental data and contribute to the understanding of indium recovery by chlorination.

2. Thermodynamic analysis

The variation of Gibbs free energy (kcal/mol of In_2O_3) as a function of temperature (°C) is shown in Fig. 1. These calculations were done using the software HSC Chemistry for Windows [10]. The reactions taken into consideration were the following:

$$In_2O_3(s) + 3Cl_2(g) \rightarrow 2InCl_3(s) + 3/2O_2(g) \quad (1)$$

$$In_2O_3(s) + 3Cl_2(g) \rightarrow 2InCl_3(g) + 3/2O_2(g) \quad (2)$$

$$In_2O_3(s) + 3Cl_2(g) \rightarrow In_2Cl_6(g) + 3/2O_2(g) \quad (3)$$

Data in Fig. 1 indicate that In_2O_3 chlorination with Cl_2 is possible throughout the temperature range considered. The products of the reaction are solids under 500 °C and gaseous at high temperatures.

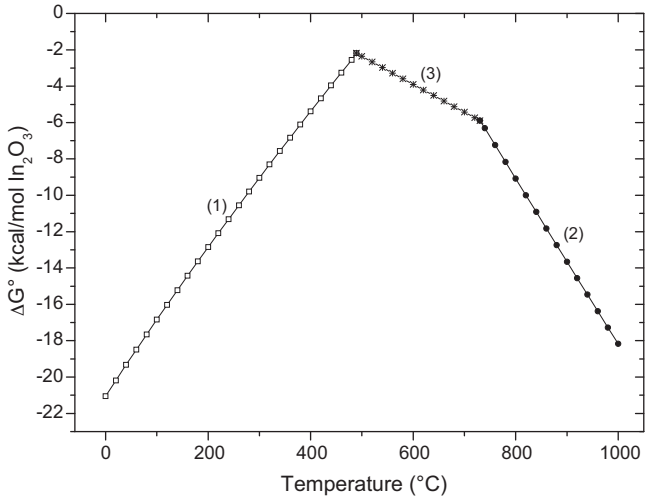

Fig. 1. Variation of Gibbs free energy vs. the temperature for In_2O_3 chlorination.

Between temperatures of 500 and 730 °C the most probable product is the species $In_2Cl_6(g)$.

To make the thermodynamic calculations presented in Fig. 1, an amount of Cl_2 enough to complete the chlorination reaction was considered. The experimental system used, while working with Cl_2, corresponds to a system where the gaseous reactive is found in excess. However, at the initial stage of the reaction, or when the chemical reaction is fast and Cl_2 diffusion is the controlling stage, the gaseous reactive can be found in defect in the reaction zone. A thermodynamic calculation considering chlorine in defect showed a low tendency to form species InCl and Cl_2, being favoured the

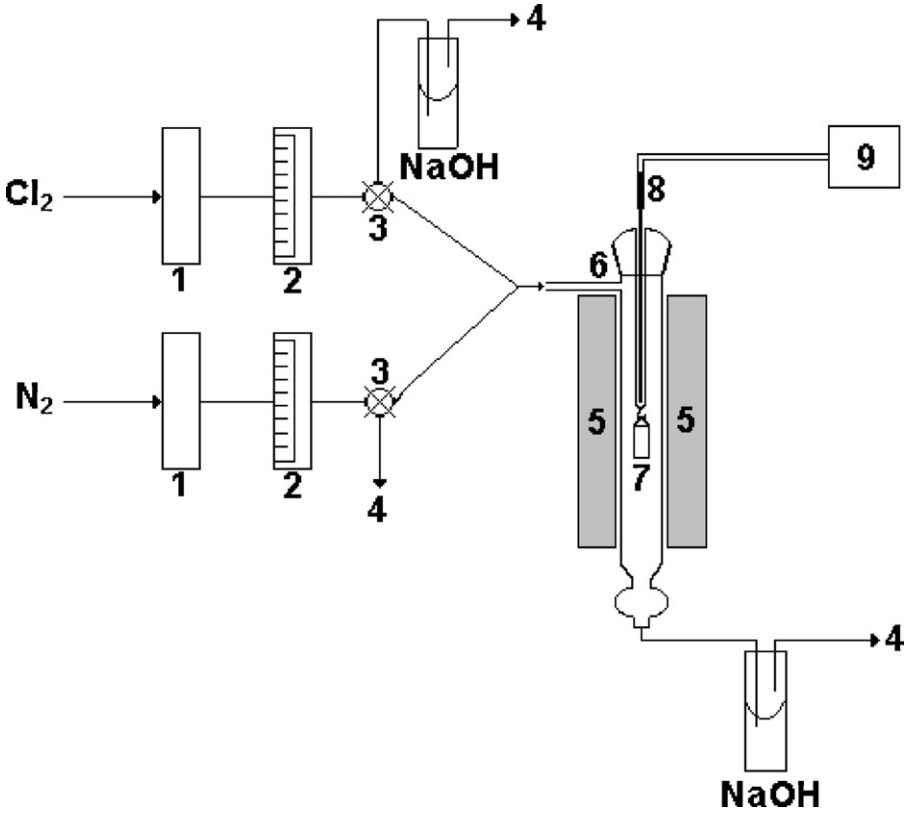

Fig. 2. Diagram of the experimental equipment: (1) drying units; (2) flowmeters; (3) 3-way valves; (4) venting; (5) furnace; (6) quartz reactor; (7) quartz crucible; (8) thermocouple; (9) temperature control unit.

formation of $InCl_3$ even when the amount of Cl_2 is much inferior to the stoichiometric.

3. Experimental

3.1. Equipments

The chlorination experiments of In_2O_3 were carried out using a tubular reactor manufactured in quartz, whose scheme is shown in Fig. 2. This reactor allows to work in atmosphere of pure chlorine.

Microstructural analysis of reactant solid species was performed by X-ray diffraction (XRD) using a Rigaku D-Max IIIC diffractometer, operated at 35 kV and 30 mA, employing Ni filter and Kα of Cu, λ = 0.15148 nm, and by scanning electronic microscopy (SEM) with a Philips Electronic Instruments SEM 515 and a LEO 1450VP equipped with an spectrometer EDAX Genesis 2000.

3.2. Materials

The gases used were 99.9% pure chlorine (Indupa, Argentina) and 99.9% pure nitrogen (A.G.A., Argentina). Fluka Chemika, 99.99% purity In_2O_3 was used in all chlorination assays. The result of the characterization of this oxide through SEM is presented in Fig. 3 and their diffractogram is matched with the file N° 6-416 [11]. Fig. 3a–c shows that the solid is made up of particles of different sizes that vary from 3 to 50 μm. It can also be observed that, at the same time, these particles are conglomerates of little grains, uniform in size, under 1 μm.

3.3. Experimental procedure

Isothermal and non-isothermal experiments, to study the effect of the temperature, reaction time, chlorine flow and partial pressure, were carried out.

The chlorination reaction of In_2O_3 was followed measuring the mass changes of the sample in each experimental assay. To do this, the masses of the sample and sample holder were previously determined and the mass of the residue was determined after each experiment so as to know the mass changes as a function of each studied variable.

3.3.1. Non-isothermal assays

The sample chlorination was performed at a set temperature and for a fixed time period of 10 min. Once the assay had finished, the reactor was purged with N_2 and the sample was weighed. Subsequently, chlorination was repeated at a higher temperature. The same flow and mass conditions as in isothermal experiments were used. The temperature increase between each point was 25 °C

3.3.2. Isothermal assays

A sample of known mass, approximately 70 mg, was supported on a quartz crucible and placed into the reaction zone, under N_2 flow until reaching the working temperature. The temperature of the reaction was obtained placing the thermocouple close the sample bed. Once the conditions selected for the experiment had been set, the three way valves were turned so that N_2 was sent to venting and pure Cl_2 or the Cl_2–N_2 mixture was let into the reactor. At that point, the starting time was recorded. After the reaction time, the reactor was purged with N_2 current. The total flow of gas, Fv, was always 100 ml/min. The residue remaining in the crucible was cooled and weighed in order to determine sample mass changes.

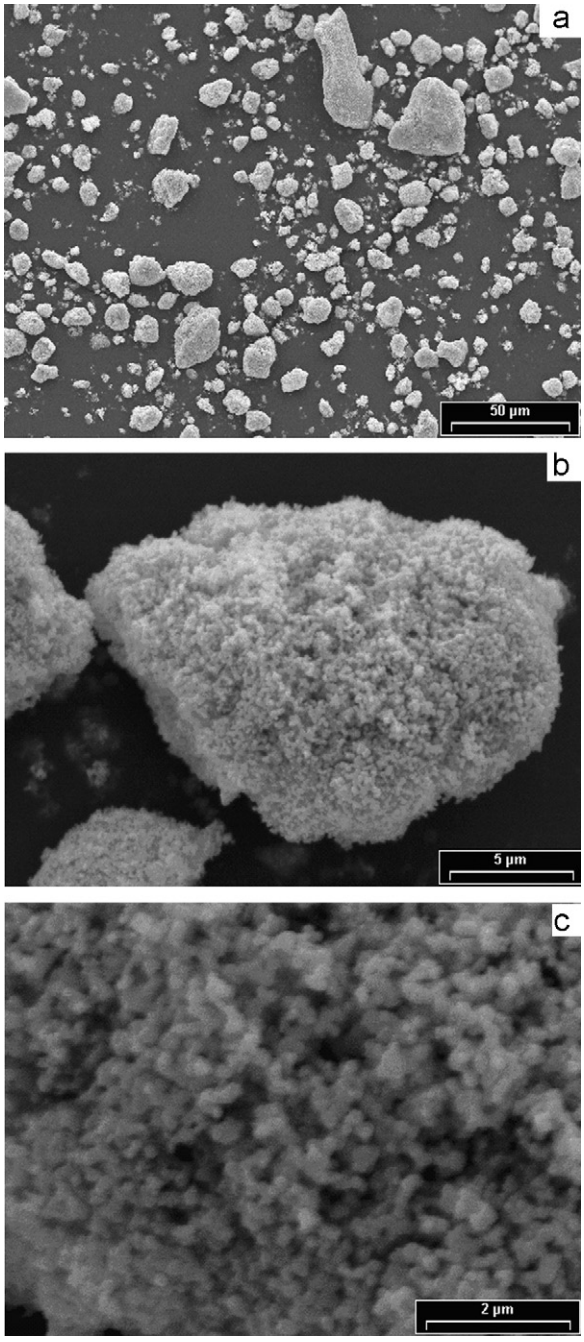

Fig. 3. Morphology of the In_2O_3 particles: (a) overall view; (b) morphology of particles of different sizes; (c) superficial appearance of a conglomerate of grains.

The mass loss suffered by the samples during non-isothermal experiments was expressed as mass loss percent, $\Delta m\%$, according to the following equation:

$$\Delta m\% = \frac{m_f - m^\circ}{m^\circ} \times 100 \quad (4)$$

The results of isothermal experiments were expressed as the degree of conversion of the solid reagent, defined as:

$$\alpha = \frac{m^\circ - m_f}{m^\circ} \quad (5)$$

where m° and m_f are the initial and final masses of In_2O_3, respectively.

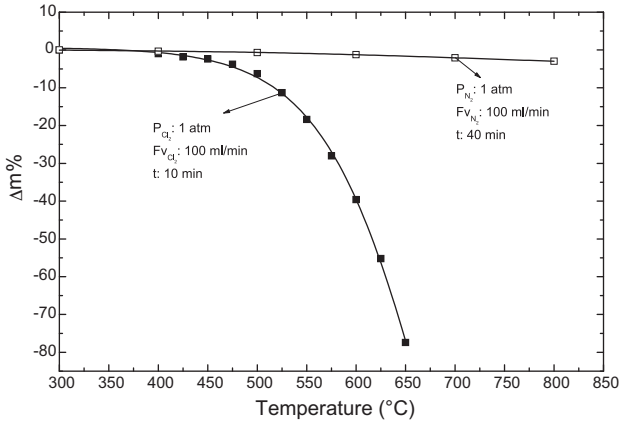

Fig. 4. Non-isothermal chlorination of In_2O_3 in Cl_2 atmosphere.

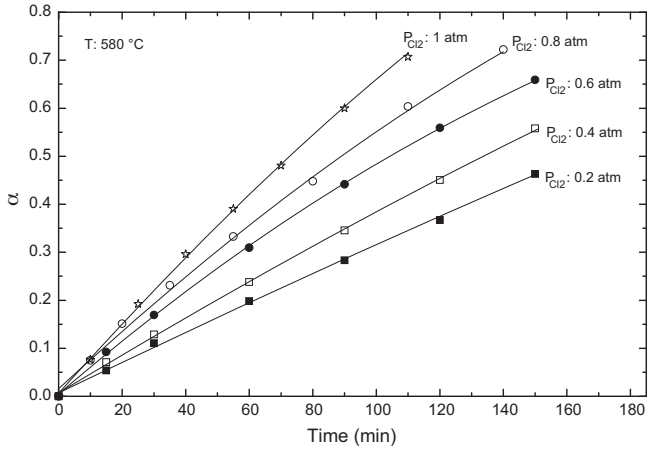

Fig. 6. Effect of Cl_2 partial pressure on the chlorination of In_2O_3.

4. Results and discussion

4.1. Non-isothermal assays

The experimental results for the non-isothermal chlorination of indium oxide are shown in Fig. 4. In the same figure, with comparative purposes, the mass loss percent in N_2 has been included.

It can be observed from Fig. 4 that the mass loss in N_2 is negligible and that the direct chlorination of In_2O_3 begins at 400 °C, reaching a mass loss of 80% at 650 °C.

4.2. Isothermal assays

The isothermal chlorination experiments of In_2O_3 were carried out to establish the kinetic parameters. The effects of temperature and partial pressure were studied.

4.2.1. Effects of temperature

The influence of temperature was investigated in the range from 500 to 650 °C. The results have been expressed as conversion vs. time, and are shown in Fig. 5. In this figure, it can be observed that a noticeable increase on the reaction rate is produced with the increase of temperature.

4.2.2. Effect of chlorine flow and partial pressure

The study of the effect of the chorine flow rate, without dilution, was performed in an interval between 50 and 200 ml/min. There were no appreciable changes in In_2O_3 conversion in the studied range.

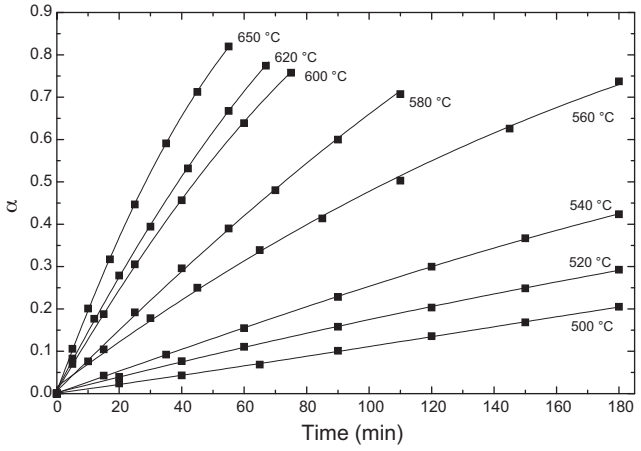

Fig. 5. Chlorination of In_2O_3 at different temperatures.

The study of the effect of chlorine partial pressure over the chlorination reaction rate of In_2O_3 was carried out by diluting the Cl_2 with N_2. The assays were performed at atmospheric pressure, keeping the total flow rate constant at 100 ml/min. Cl_2 partial pressures of 0.2, 0.4, 0.6, 0.8, and 1 atm were investigated at a working temperature of 580 °C. Fig. 6 shows an appreciable variation of the system reactivity with Cl_2 partial pressure.

4.3. Characterization of the reaction residues

SEM micrographs of the residues of In_2O_3 chlorination are shown in Fig. 7a–c. The comparison between Figs 3 and 7 show that, in general, the particles have maintained their shape and diminished their size. When comparing Fig. 3b and c with Fig. 7a–c desegregation of the particles and grains that form the agglomerates can be observed.

The XRD analysis of the chlorination residues obtained under different experimental conditions did not show changes in the crystalline structure of In_2O_3. Likewise, no chlorinated compounds were detected by XRD in the residue.

4.4. Kinetic models and mechanism of reaction

It is known that the rate of heterogeneous reactions depends on the surface of the solid reactant. Therefore, it is necessary to establish functions that link the particle size with the progress of the reaction [12–14]. A general function for the different types of particles is represented by Eq. (6):

$$1 - (1 - \alpha)^m = \mathrm{Kt} \tag{6}$$

where the exponent m can vary between 1 (particles in plate form) and 1/3 (spheric particles), and the constant K depends on different parameters, among which it is found a kinetic constant, k, which at the same time depends on the temperature according to the Arrhenius expression:

$$k = Ae^{-E/RT} \tag{7}$$

The results of experimental data adjustment of the chlorination of In_2O_3, at different temperatures, with the model given by Eq. (6) are shown in Fig. 8, for $m = 0.4$, i.e. the shape of the particles can be considered halfway between cylinders $m = 1/2$ and spheres $m = 1/3$. In this figure it can be observed that the correlation between the experimental results and the predicted values for the kinetic model is excellent.

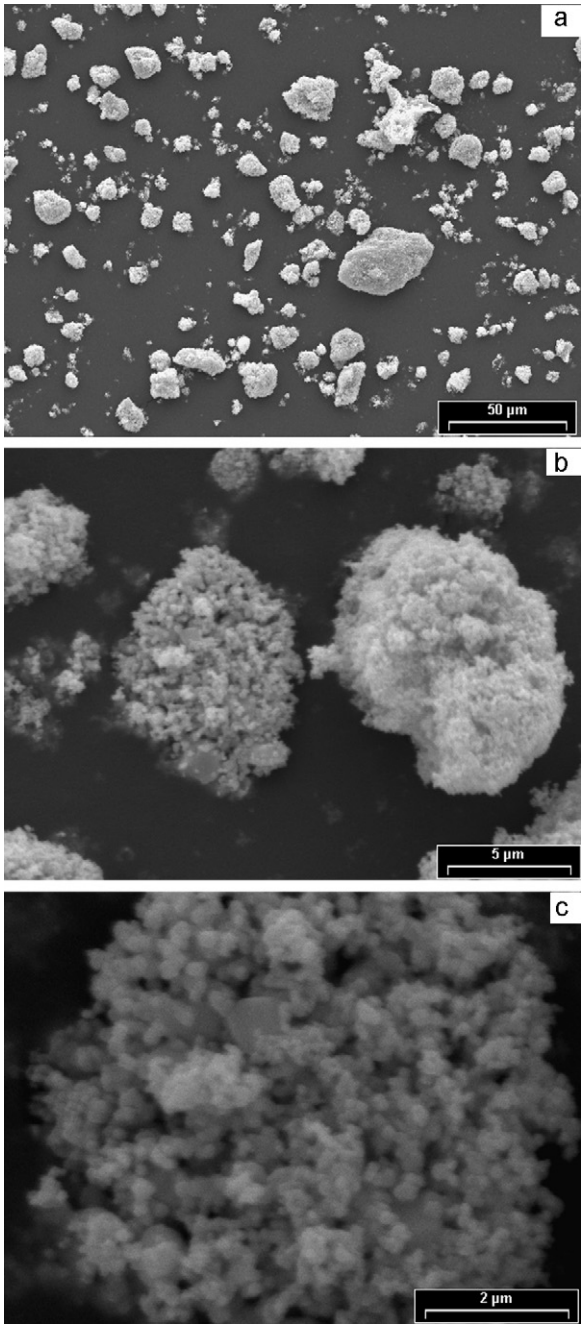

Fig. 7. SEM analysis of the chlorination residue at 580 °C: (a) overall view of a chlorinated residue; (b) attacked particles; (c) surface of the conglomerate after the chlorination.

The activation energy was calculated from a plot of $\ln K$ vs. $1/T$ since the kinetic constant k is directly proportional to the constant K of Eq. (6). In Fig. 9 the results obtained are presented. The estimated activation energy value suggests that the chlorination reaction rate is controlled by the superficial chemical reaction between the Cl_2 and the In_2O_3.

The apparent order of reaction with regards to the partial pressure of chlorine was estimated from a graphic of $\ln K$ vs. $\ln PCl_2$ (Fig. 10), which was built by applying the kinetic model provided by Eq. (6) to the curves in Fig. 6.

Fig. 10 shows that, for the partial pressure intervals of Cl_2 between 0.6 and 1 atm, the experimental points tend to order in a line with a slope value close to 1. At lower values of the partial pressure of Cl_2 a change in the slope is produced, what means that

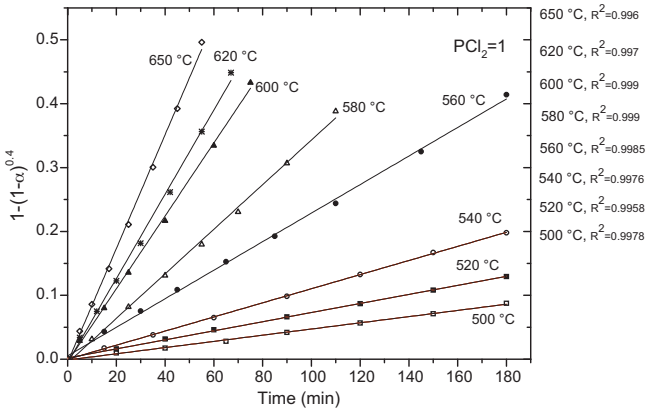

Fig. 8. Mathematical fit of the experimental data of In_2O_3 chlorination at different temperatures. (—) Kinetic model; (●) experimental data.

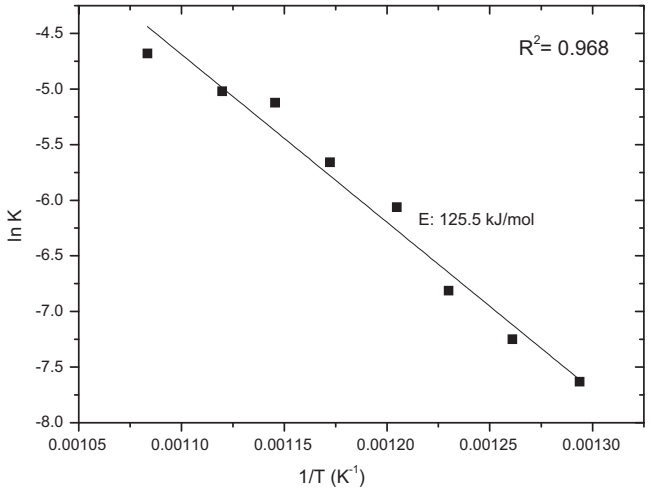

Fig. 9. Arrhenius plot for the chlorination of In_2O_3.

when varying PCl_2 in a given interval, the reaction order is modified. A variation of the apparent order of reaction with regards to the partial pressure of chlorine has been observed in other chlorination systems [15–17] and it can be attributed to several factors, such as the diffusive effects that could control the rate reaction at low chlorine partial pressures. Furthermore, it has been proved by González et al. [18,19] that the chlorination reactions, mainly of metallic oxides, occur through a reversible reaction, in which

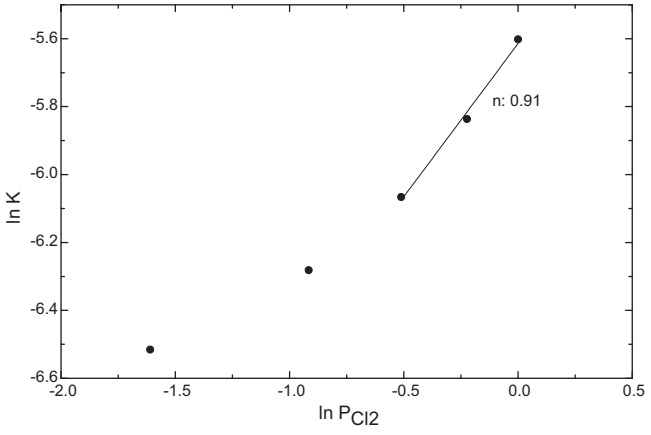

Fig. 10. Estimation of the order of reaction between 0.6 and 1 atm.

the results of the reaction, metallic chlorides and oxygen, can react among themselves in a gaseous phase to form an oxide, which could be the same as in the beginning or be at a different phase. This phenomenon is revealed in a morphological change of the particles. A detailed observation of Fig. 7c shows that among the grains from the attacked particle, some are bigger in size and have different habits from the originals. This is consistent with what was observed in other systems [18,19] and it is attributed to the reversibility of the chlorination reaction, thus some grains grow because of the reaction at the gaseous phase between the chlorination products. This phenomenon, which according to Fig. 7c would happen in this system, can vary in the function of chlorine concentration and be another cause for the nonlinearity of Fig. 10.

When the chlorine concentration is low and a flow system like the one used in this work is used, mostly all of the chlorination products are removed from the reaction zone, and hence, the reversibility of the reaction can be negligible. This and the apparent order of reaction with regards to the partial pressure of chlorine, found experimentally at high Cl_2 partial pressures, may suggest that the chlorination process of In_2O_3 occurs through a direct reaction. Two stages could be involved in this reaction: a slow stage that controls the reaction rate and a fast stage.

$$In_2O_3(s) + Cl_2(g) \rightarrow 2InOCl + 0.5O_2(g) \quad \text{(slowstage)} \quad (8)$$

$$2InOCl + 2Cl_2(g) \rightarrow 2InCl_3(g)/In_2Cl_6(g) + O_2(g) \quad \text{(faststage)} \quad (9)$$

The mechanism proposed in reactions (8) and (9) for the chlorination of In_2O_3 in the studied temperature range implies, as a first step, the formation of InOCl, species that has been identified by other authors [8,20]. This reaction is followed by a fast chlorination stage where $InCl_3(g)$ or $In_2Cl_6(g)$ is formed. The presence of the dimeric form $In_2Cl_6(g)$ has been observed in the vapor when $InCl_3(s)$ is vaporized at high temperature [21].

The compound InOCl has been characterized previously by other authors who studied a process of obtaining In_2O_3 from $InCl_3$ in an aqueous solution [20]. They found that InOCl is stable up to 350 °C with an orthorhombic structure and decomposes at higher temperatures.

To assume that the stage (8) is slow and (9) is fast, may explain why InOCl was not detected by XRD and no mass increase of the reacting solid due to the formation and deposition of InOCl, was observed. A similar mechanism has been proposed by Milne [22] for the chlorination of bauxite.

5. Conclusions

The chlorination of In_2O_3 with gas Cl_2 starts to be significant for temperatures higher than 400 °C.

The value found for the apparent activation energy, 125.5 kJ/mol, indicates that the chemical stage performs an important role on the control of reaction rate.

The fitting to different kinetic models showed that the experimental data are well represented by equation $1-(1-\alpha)^m = Kt$, with $m = 0.4$.

The results of the estimation of the apparent order of reaction with regards to the partial pressure of chlorine indicate that at high Cl_2 partial pressure the reaction mechanism responds to reactions (8) and (9), where reaction (8) corresponds to the controlling stage of the reaction rate.

Acknowledgements

This work was supported by Universidad Nacional de San Luis, Fondo para la Investigación Científica y Tecnológica (FONCyT) and Consejo Nacional de Investigaciones Científicas y Técnicas, Argentina.

References

[1] F.A. Cotton, G. Wilkinson, C.A. Murillo, M. Bochmann, Advanced Inorganic Chemistry, John Wiley and Sons, New York, 1999.
[2] F. Habashi, Handbook of Extractive Metallurgy, Vol. III, Whiley-VCH, Wienheim, 1997.
[3] J.E. Hoffmann, Advances in the extractive metallurgy of selected of rare and precious metals, J. Operations Manage. 43 (1991) 18–23.
[4] H. Ohwa, M. Yukinobu, J. Nabeshima, M. Yasukawa, High-purity metals production of Sumitono Metal Mining Co., Ltd, Extr. Metal. Inst. Min. Metal. 89 (1989) 885–898.
[5] S. Nishihama, T. Hirai, Isao Komasawa, Separation and recovery of gallium and indium from simulated zinc refinery residue by liquid–liquid extraction, Ind. Eng. Chem. Res. 38 (1999) 1032–1039.
[6] P.K. Jena, E.A. Brocchi, Metal extraction through chlorine metallurgy, Miner. Process. Extr. Metal. Rev. 16 (1997) 211–237.
[7] H. Takahashi, K. Suguwara, R. Nonoka, Recovery of indium from ground powder by chlorination and solvent extraction, Kagaku Kogaku Robunshu. 34 (5) (2008) 527–532.
[8] W. Kye-Sung Park, G. Sato, T. Grause, T. Kameda, Yoshioka, Recovery of indium from In_2O_3 and liquid crystal display powder via a chloride volatilization process using polyvinyl chloride, Thermochim. Acta 493 (2009) 105–108.
[9] O. Terakado, T. Saeki, R. Irizato, M. Hirasawa, Pyrometallurgical recovery of indium from dental metal recycling sludge by chlorination treatment with ammonium chloride, Mater. Trans. 51 (6) (2010) 1136–1140.
[10] A. Roine, Outukumpu HSC Chemistry for Windows, Version 5.1, Outokumpu Research, Pori, Finland, 2003.
[11] Card N(6-416 of JCPDS, Powder Difraction Files, 1993.
[12] F. Habashi, Principles of Extractive Metallurgy, Gordon and Breach Science Publishers Inc., New York, 1980.
[13] O.D. Quiroga, J.R. Avanza, A.J. Fusco, Modelado Cinético de las Transformaciones Fluido-Sólido Reactivo, Editorial Universitaria de la Universidad del Nordeste (EUDENE), Argentina, 1996.
[14] O. Levenspiel, Ingeniería de las Reacciones Químicas, Editorial Reverté S.A, Buenos Aires, 1976.
[15] A.C. Bidaye, S. Venkatachalam, C.K. Gupta, Studies on the chlorination of zircón. Part I. Static bed investigations, Metal. Mater. Trans. B. 30B (1999) 205–213.
[16] P.K. Jena, O. Barbosa-Filho, I.C. Vasconcelos, Studies on the kinetics of slurry chlorination of a sphalerite concentrate by chlorine gas, Hydrometallurgy 52 (1999) 111–122.
[17] J.A. González, J.B. Rivarola, M. del, C. Ruiz, Kinetics of chlorination of tantalum pentoxide in mixture with sucrose carbon by chlorine gas, Metal. Mater. Trans. B 35B (2004) 439–448.
[18] J. González, M. del, C. Ruiz, J.B. Rivarola, D. Pasquevich, Effects of heating in air and chlorine atmosphere on the crystalline structure of pure Ta_2O_5 or mixed with carbon, J. Mater. Sci. 33 (1998) 4173–4180.
[19] J. González, M. del, C. Ruiz, D. Pasquevich, A. Bohé, Formation of niobium–tantalum pentoxide orthorhombic solid solutions under chlorine-bearing atmospheres, J. Mater. Sci. 36 (2001) 3299–3311.
[20] Heqing Yang, Hua Zhao, Hongxing Dong, Wenyu Yang, Dichun Chen, Preparation of In_2O_3 octahedrons by heating $InCl_3$ aqueous solution on the Si substrate, Mater. Res. Bull. 44 (2009) 1148–1153.
[21] B. Brunetti, V. Piacente, P. Scardala, A torsion study on the sublimation process of $InCl_3$, J. Chem. Eng. Data 43 (1998) 101–104.
[22] D. Milne, The chlorination of alumina and bauxite with chlorine and carbon monoxide, Proc. Aust. Inst. Miner. Metal. 260 (1976) 23–31.